



# Fabrication of gelatin nanofiber webs via centrifugal spinning for N95 respiratory filters

FATIH ARICAN<sup>1,2,\*</sup> , AYSEGUL UZUNER-DEMIR<sup>1,3</sup>, OGUZHAN POLAT<sup>1</sup>,  
AYKUT SANCAKLI<sup>1,4</sup> and EZGI ISMAR<sup>1</sup>

<sup>1</sup>Kazlicesme R&D Center and Test Laboratories, 34956 Tuzla, Turkey

<sup>2</sup>Department of Chemistry, Sakarya University, 54050 Serdivan, Turkey

<sup>3</sup>Department of Polymer Science and Technology, 41000 Kocaeli, Turkey

<sup>4</sup>Department of Leather Engineering, Ege University, 35040 Izmir, Turkey

\*Author for correspondence (fatiharican@kazlicesme.com.tr)

MS received 4 October 2021; accepted 28 December 2021

**Abstract.** Due to the impact of the Covid-19 pandemic, the usage of numerous protective face masks has faced an explosion in demand around the world. Therefore, the need to reduce the environmental pollution caused by disposable single-use face masks has become vital. Recently, alternative raw material solutions have been discussed to eliminate the consumption of single-use plastics. Within this research, gelatin nanofibers were fabricated via centrifugal spinning technique, and filtration media were investigated in terms of air permeability and filtration efficiency. In addition, morphological properties were examined with scanning electron microscopy. Fabricated fibers have a changing average diameter range from 232 to 778 nm, and targeted 95% filtration efficiency was achieved in several compositions. It was proven that biodegradable gelatin nanofibers could be a sustainable alternative for disposable N95 respiratory filters.

**Keywords.** Gelatin; centrifugal spinning; N95; mask; filter.

## 1. Introduction

Protective face masks have been proposed as a potential tool to combat the COVID-19 outbreak since the first epidemic outbreak [1]. According to the World Health Organization (WHO) report, as of 7 July 2021, 184,324,026 cases have been confirmed, and 3,992,680 people have lost their lives [2]. Later, all countries globally have been encouraged for the usage of masks as part of the fight against Covid-19. In this context, the use of N95 masks with particle retention efficiency of 95% and above has increased. However, there is still a shortage of N95 masks in various parts of the world [3].

Properties of the N95 facemask are defined as at least 95% filtering efficiency to particles with a median diameter >0.3  $\mu\text{m}$  and protects from respiratory droplets, where N signifies that the mask is not resistant to oil [4]. NIOSH (National Institute of Occupational Safety and Health), European EN149, N95 mask and EN ISO 9237 Standards create the specifications necessary to produce masks. For respiratory filters, nonwovens and nanofiber webs are preferred layers. Nanofibers are one of the best alternatives for the mask due to their distinct features, including the higher surface area, which can be functionalized for desired property, uniform morphology, and consistency in structural properties.

Nanofibers are an important class of materials used in various fields such as filtration, tissue engineering, protective suits, energy storage, etc. [5,6]. Although electrospinning is one of the most used methods to produce nanofibers, its commercial use is limited due to its low production speed and appropriateness of a limited number of materials. Centrifugal spinning, a newly developed method for producing nanofibers, has unique advantages such as low cost, fast production, a wide selection of materials, and is independent of the electric field compared to electrospinning [7]. The centrifugal spinning method is based on spraying the spinning solution from the spinneret during the spinning process. The direct current motor generates the centrifugal force, and when the centrifugal force is over, the surface tension of the liquid fiber formation will be achieved. The jet then undergoes a stretching process via rapid evaporation of the solvent, and dried nanofibers are accumulated on the collectors [8].

Gelatin is a gelling protein that is a denaturated form of collagen, and according to extraction type (acidic or alkaline), it is named Type A or Type B [9]. Gelatin can be obtained from the skin, bones, cartilage of marine animals and mammals [10]. The most common source of gelatin is bovine and porcine, and the quality of gelatin is generally defined with its bloom strength [11]. The chemical structure of gelatin consists of Gly-X-Y amino acid sequence and

multiple repetitions of it, which is similar to collagen, where X refers to Proline (Pro) and Y refers to hydroxyproline (Hyp) [12]. Gelatin has a wide range of applications from biomedical to cosmetics, food to pharmaceutical [13–15]. Gelatin is a natural biopolymer with a good film-forming ability and a wide range of application areas; however, fiber formation of gelatin with conventional wet and dry spinning techniques is inadequate [16,17]. Synthetic filter media usage has drawbacks when they come to their end-of-life cycle for disposal issues and pollution. Biodegradable materials are a good alternative for filtration materials. Gelatin nanofibers can be an alternative for synthetic respiratory filter media for filtration [18,19]. Thus, centrifugal spinning can be a good alternative to fabricate submicron gelatin fibers [20,21].

In this study, we develop an alternative filter media to replace synthetic surgical mask filters with gelatin nanofiber webs, which are successfully fabricated via centrifugal spinning technique. The air permeability, pore size, filtering efficiency and handling properties of the filter media are compared with commercial masks. Results indicated that gelatin nanofiber webs could be a good alternative for synthetic filtration media and used as N95 respiratory masks.

## 2. Materials and methods

Acetic acid (AA;  $\geq 99.5\%$ ;  $60.05 \text{ g mol}^{-1}$ ) and formic acid (FA;  $\geq 95\%$ ;  $46.02 \text{ g mol}^{-1}$ ) were purchased from Sigma Aldrich and used as-received. Commercially available food grade type B bovine gelatin was purchased from Halavet Gelatin, Turkey.

Fabricated gelatin nanofiber webs were observed using scanning electron microscopy (SEM; model MA10, Zeiss, Germany). The nanofiber diameters between the gelatin fibers were measured based on the SEM images using ImageJ software. Structural analysis of the gelatin nanofibers was conducted via Fourier transform infrared spectrometer (FTIR, model Cary 630, Agilent, USA). Air permeability measurements were collected using Prowhite Airtest II (Istanbul, Turkey) permeability measurement device. All analyses were carried out according to EN ISO 9237 standards, at  $22 \pm 2^\circ\text{C}$ , 100 Pa and  $20 \text{ cm}^2$  test conditions. Filtration efficiency was measured with Proser K008 (Istanbul, Turkey). The test standard applied in all analyses is NaCl,  $0.3 \mu\text{m}$ ,  $15.8 \text{ cm s}^{-1}$  and  $95 \text{ l min}^{-1}$ .

### 2.1 Experimental design

Response surface methodology (RSM) is a compilation of mathematical and statistical methods that help fit the models and analyse the problems, in which many independent parameters control the dependent parameters [22]. In this study, RSM experimental modelling method was applied.

Furthermore, Minitab 17 was used for statistical analysis. Thus, it is aimed to reach the optimum process parameters with a lower number of experiments. In this context, the RSM experimental modelling method was applied to produce nanofibers from natural and synthetic polymers and their combined experiments.

### 2.2 Fabrication of gelatin nanofibers

Fabrication of the nanofibers was conducted with the centrifugal spinning machine (Nanocentrino, Areka, Turkey). Spinneret is the main component of the centrifugal spinning device. Solution was fed into spinneret, and during the process, centrifugal force overcomes the surface tension and result in the rapid evaporation of the solvent, and polymeric material stretched in between the rod collectors. Therefore, centrifugal spinning can be considered safer than electrospinning due to the lack of applied high voltage, and it is also possible to fabricate large-scale submicron fibers, thanks to the centrifugal spinning technology [23,24]. A schematic diagram of the centrifugal spinning is shown in figure 1.

Gelatin can be easily soluble in water at a temperature  $\geq 40^\circ\text{C}$ ; however, it is impossible to obtain ultra-fine submicron fibers even with electrospinning [17]. Gelatin is soluble in several acidic and organic solvents, such as AA, FA and water. AA is a suitable solvent for gelatin to fabricate a well-defined nanofibrous structure due to the lower surface tension compared with FA and  $\text{H}_2\text{O}$  [25]. Gelatin was dissolved in AA at a concentration of 10–20–30% (w/v) and mixed at  $40^\circ\text{C}$  for 30 min. In the process of centrifugal spinning, gelatin solutions were placed in plastic syringes with a needle of 22G, and the solution was fed through the spinneret at a  $25\text{--}30 \text{ ml h}^{-1}$  rate, and solution consumption was kept constant for all. Spinneret rotation speed was studied from 4000 to 8000 rpm, the rotational speed of the collector was set to 200 rpm, and the distance between the spinneret and the collector was set to 20 cm. All experiments were conducted at room temperature. The solvent was ejected under the centrifugal force, generated by a rotation, and centrifugal force causes stretching of the jets, followed by the evaporation of solvent before being collected. Gelatin solutions were prepared in different ratios. Table 1 presents the details of the fabrication process.

### 2.3 Assembly of three-layered mask structures

Nonwoven 100% polypropylene spun-bond and melt-blown fabrics have been used to obtain a three-layered mask structure (figure 2). Gelatin nanofibers obtained by centrifugal spinning were used as a filter layer, other fabrics were evaluated as inner and outer layers. Thus, fabricated nanofiber webs were laminated in between polypropylene nonwoven layers. When fabricated masks

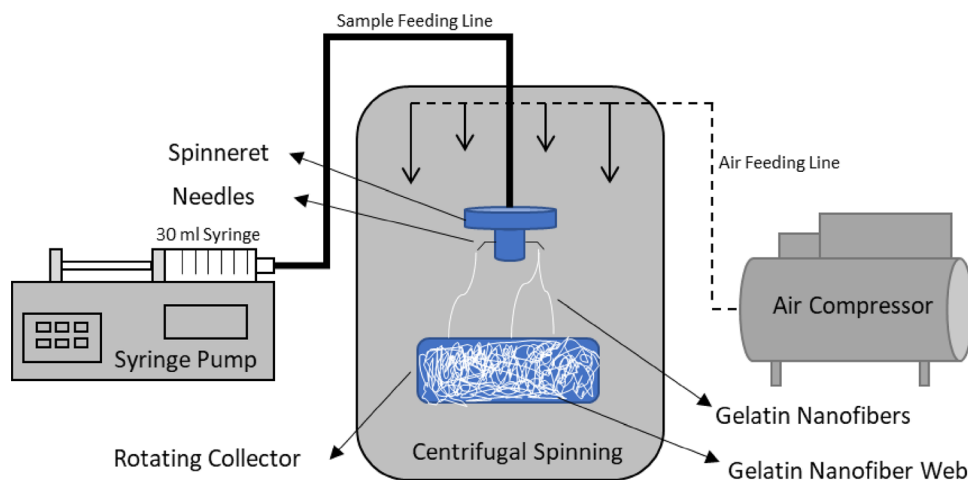


**Figure 1.** Schematic diagram of centrifugal spinning with a horizontal collector.

**Table 1.** Fabrication parameters of gelatin nanofiber webs.

Sample code	Concentration (%)	Rotational speed (rpm)	Feeding rate (ml h <sup>-1</sup> )
GEL 1	20	6000	25
GEL 2	20	8000	30
GEL 3	10	8000	30
GEL 4	10	4000	30
GEL 5	20	4000	30
GEL 6	20	6000	30
GEL 7	30	6000	25
GEL 8	10	6000	25
GEL 9	30	6000	25
GEL 10	15	6000	25

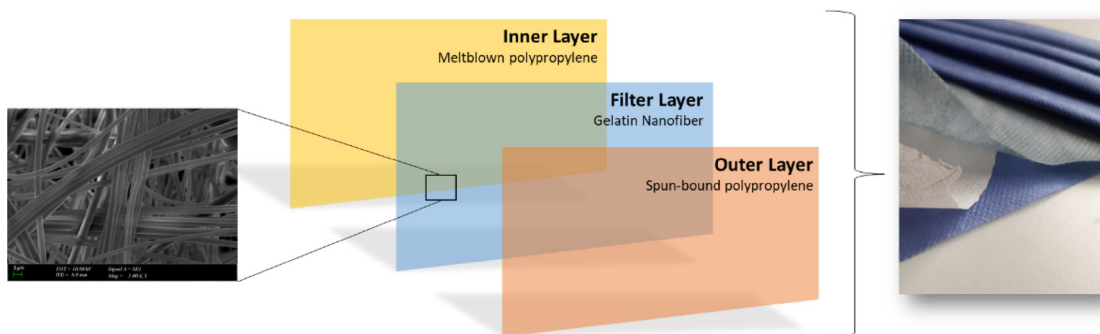


**Figure 2.** Illustration of each layer of three-layered mask structure.

were evaluated for their odour, face fitting, stripe quality and breathability, they presented similar properties to the commercial surgical masks. Specifically, the odour is one of the unwanted properties of surgical type masks, and fabricated masks with pure gelatin do not have a

disturbing odour. Also, there was no face fitting for assessed mask types, and a stripe quality problem was observed. The breathability feeling of the gelatin-containing masks presents similar properties to the commercial ones.

### 3. Results and discussions

The fiber morphology of gelatin nanofibers prepared at different concentrations, rotational speed, and feeding rate ratios were compared using SEM images (figure 3). Average fiber diameter and pore size were calculated from SEM images of the nanofiber webs. At least 50 measurements were done for each, and Image J software analysed the SEM images. The selected SEM images of gelatin nanofibers show that bead-free and entanglement-free random nanofibers are obtained. The average pore size of the nanofiber webs was changed from 0.37 to 2  $\mu\text{m}$ . Figures 3

and 4 presents the histogram of nanofiber diameter and pore size distribution, and all results with standard deviation and coefficient of variation (CV%) are presented in Table 2.

These results prove that the best fiber diameter size belongs to GEL1 (232 nm), and the parameter values where the concentration is 20%, the rotational speed is 6000 rpm, and the feeding rate is 25 ml h<sup>-1</sup> are the optimum parameters for producing gelatin/AA nanofibers. Furthermore, according to SEM results, nanofiber formation was achieved for samples without defects such as beads and stuck fibers.

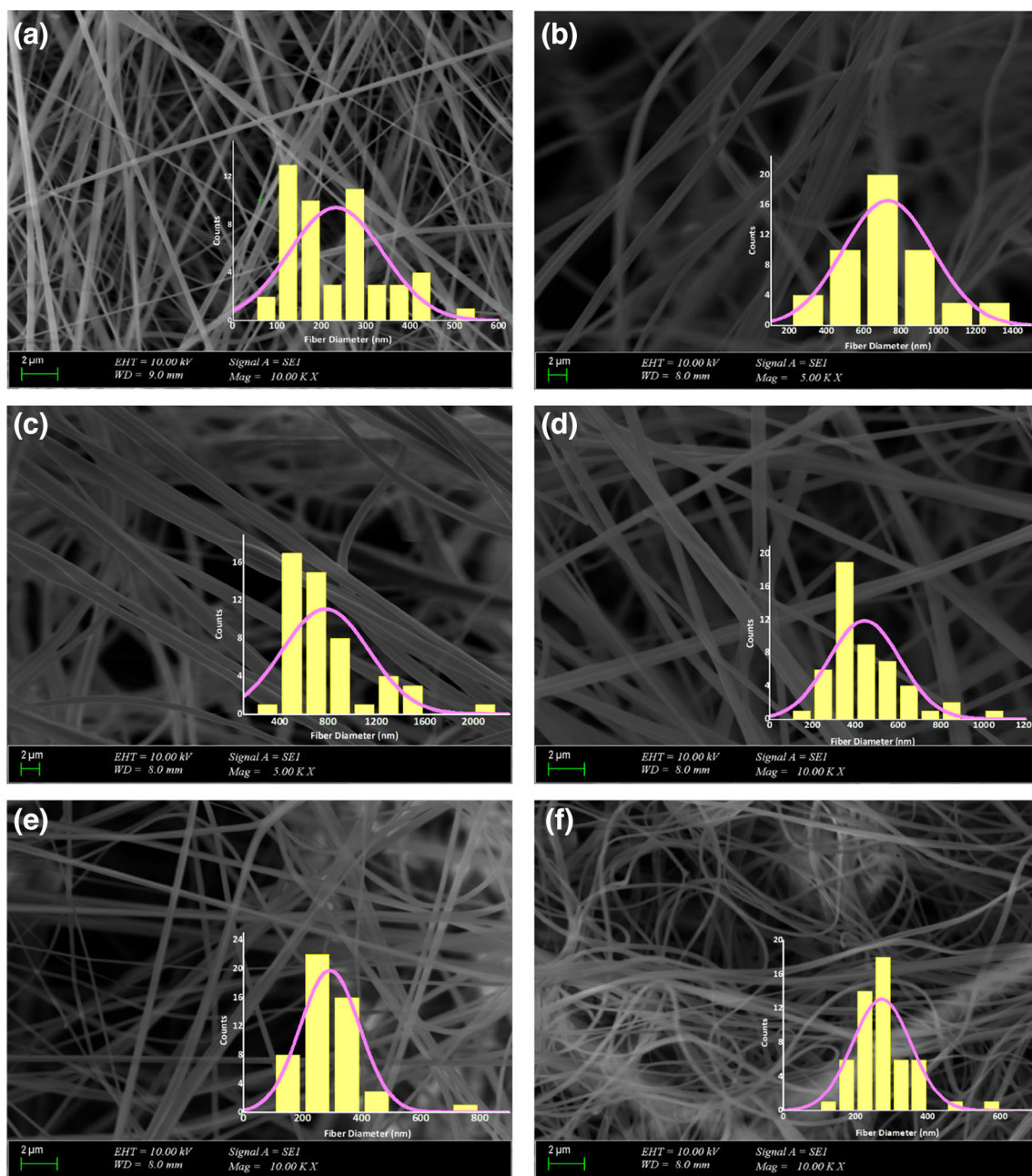


**Figure 3.** SEM images of masks: (a) GEL 1, (b) GEL 2, (c) GEL 3, (d) GEL 5, (e) GEL 6 and (f) GEL 9.



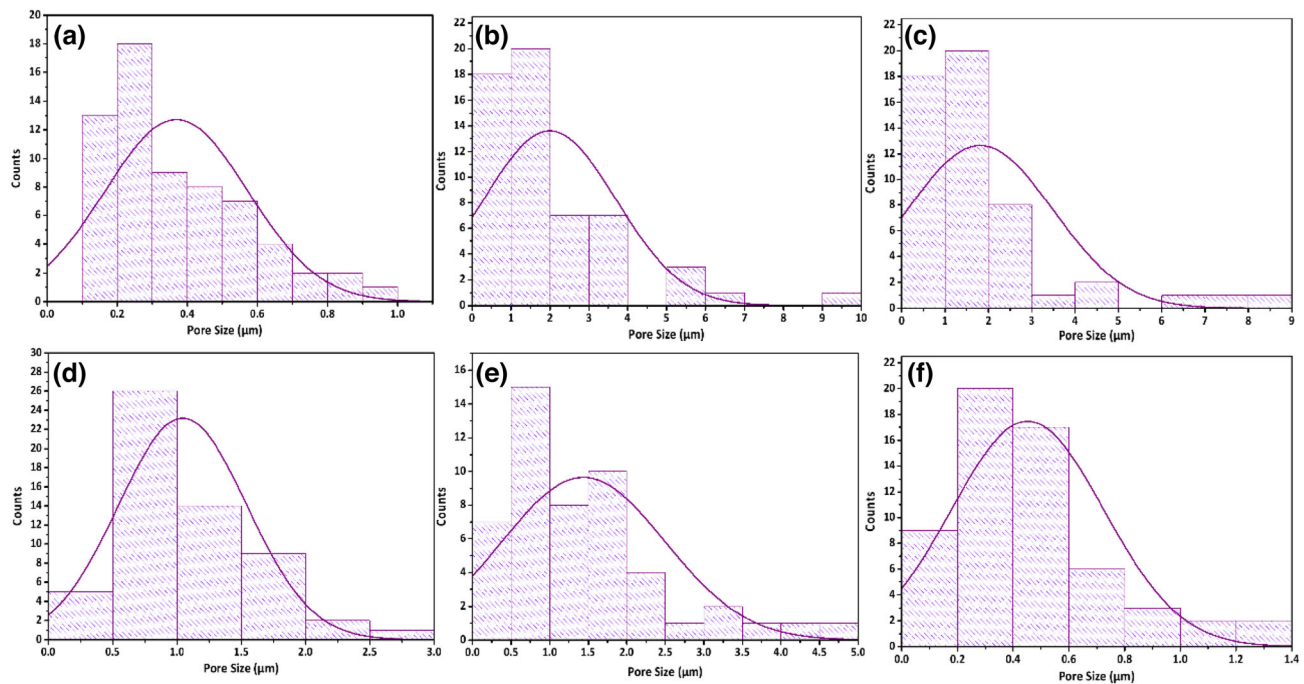


**Figure 4.** Histograms of the pore size distribution of the masks: (a) GEL 1, (b) GEL 2, (c) GEL 3, (d) GEL 5, (e) GEL 6 and (f) GEL 9.

**Table 2.** Average fiber diameter and pore size of the gelatin nanofiber webs.

Sample code	Avg. fiber diameter (nm)	Standard deviation	CV%	Avg. pore size (μm)	Standard deviation	CV%
GEL 1	232	0.11	45.69	0.37	0.20	54.05
GEL 2	728	0.24	33.10	2.00	1.70	85.00
GEL 3	778	0.36	46.14	1.81	1.67	92.26
GEL 5	442	0.17	37.78	1.04	0.50	48.08
GEL 6	292	0.10	34.59	1.44	1.05	72.92
GEL 9	272	0.08	29.78	0.45	0.27	60.00

### 3.1 Fourier transform infrared spectroscopy

For structural analysis, FTIR analysis was performed for gelatin nanofiber. FTIR spectra of gelatin powder and gelatin nanofiber webs are presented in figure 5a and they are identical. Gelatin has characteristic peaks Amide A, B, and Amide I, II and III. The peak at around  $1650\text{ cm}^{-1}$  was associated with amide I, while  $1551\text{ cm}^{-1}$  for amide II and  $1241\text{ cm}^{-1}$  for amide III. Amide I is corresponding to the stretching vibration of the C=O, amide II bending vibration of N–H bonds and stretching vibrations of C–N bonds. Amide III is related to the vibrations in the plane of C–N, and N–H groups of amides and is located around  $1241\text{ cm}^{-1}$  [26]. Amide A and B bands are located at around  $3280$  and  $2948\text{ cm}^{-1}$ , corresponding to the stretching vibration of the N–H bonds and stretching of the C–H bonds, respectively [26–31].

### 3.2 Air permeability and filtration efficiency

After the three-layered mask structures were collected as described above and filtration properties were evaluated, the filtration efficiency tests of the three-layered mask prototypes created with the produced nanofiber covers were carried out with the automated filter tester TSI 8130A. Filtration efficiency ( $\eta$ ) and pressure drop ( $\Delta P$ ) values were obtained from the automated filter tester device. The measurement samples with an effective area of  $100\text{ cm}^2$  were tested against the NaCl aerosols at a face velocity of  $15.83\text{ cm s}^{-1}$ . Pressure drop through the nonwoven fabric sample was measured via sensors. Figure 5b presents the schematic description of the experimental setup.

Filtration efficiency ( $\eta$ ) was calculated according to equation (1), where  $C_{\text{down}}$  and  $C_{\text{up}}$  present downstream and

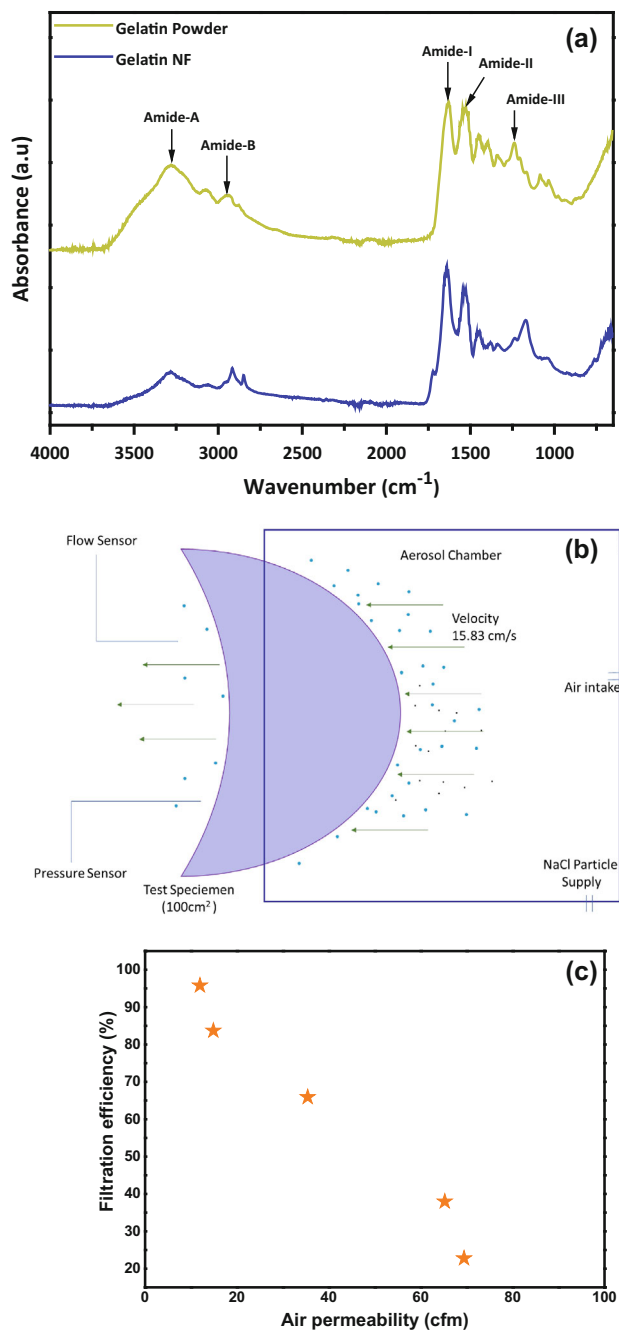


**Figure 5.** (a) FTIR spectra of gelatin powder and gelatin nanofiber. (b) Schematic diagram for the filtration efficiency. (c) Relationship between filtration efficiency and air permeability.

upstream particle concentrations, respectively [32]. The automated filter tester was collected to  $C_{down}$  and  $C_{up}$  data.

$$\eta = 1 - \frac{C_{down}}{C_{up}} \quad (1)$$

We aim to reach at least 95% filtration efficiency for our eco-design mask model to reach N95 respiratory filter properties. For sample GEL 1, the filtration efficiency value was above 95%. Mask samples consisted of three layers of

nonwovens. Measurements were conducted for the samples without containing GEL nanofiber web, only a double layer of the mask was analysed. For 2 nonwoven layers, filtration efficiency and air permeability values were 5.86% and 91.08 cfm, respectively. Figure 5c gives the relationship between air permeability and filtration efficiency for fabricated gelatin nanofiber masks. As seen from the figure, filtration efficiency and air permeability present inverse proportions. Filtration efficiency and the pressure drop are significant parameters while defining the performance of the face mask [33]. For this reason, a parameter called the filtering quality factor has been introduced to take an account of both parameters [34].

The quality factor ( $Q$ ), which is a measure of mask performance, is calculated using equation (2). Where  $\Delta P$  is the pressure drop and  $\eta$  the filtration efficiency.

$$Q = -\frac{\ln(1-\eta)}{\Delta P} \quad (2)$$

As a result of the calculation, the quality factor values of samples were found as 11.153, 7.371, 9.22, 8.373 and 10.667 kPa<sup>-1</sup> for Gel 1, Gel 3, Gel 4, Gel 8 and Gel 9, respectively.

### 3.3 Statistical analysis

A one-way analysis of variance method was applied to understand any difference between the three groups regarding specific-dependent measures. Tukey test, a statistical test, is a one-step multiple comparison procedure. Therefore, it can be applied to the entire set of pairwise comparisons simultaneously to find data that differ significantly from each other [35]. Minitab calculates that Tukey's method entries set of comparisons should have a family error rate of 0.05 (equivalent to a 95% simultaneous confidence level) [36]. With this context, it is possible to examine the confidence intervals and whether any of them contain zero, whether there is a significant difference [37].

Figure 6 shows the effect of concentration and rotational speed on filtration efficiency with contour and surface plot. It is seen that the highest filtration efficiency was reached in the concentration range of 20–25% at an average rotation speed of 6000–7000 rpm.

As seen in figure 7, the effect of concentration and rotational speed on air permeability was examined with contour and surface plots. In this context, we can say that the highest air permeability values are achieved at low concentration and low rotational speeds. We assume that this reason is due to the inability to produce enough fiber under fabrication conditions. As a result, the optimum concentration and rotational speed are 20–25% and in the range of 6000–7000 rpm, respectively.

Figure 8a presents the optimum process parameters to reach 95% filtration efficiency. According to analysis results, 20% concentration and around 6000 rpm are ideal

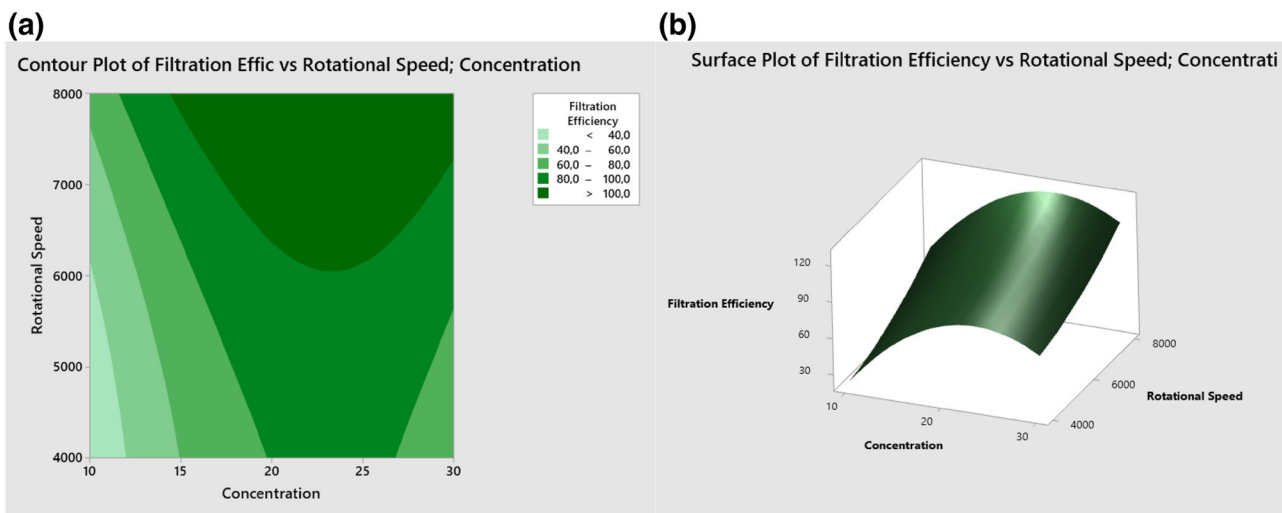


Figure 6. The effect of concentration and rotational speed on filtration efficiency: (a) contour plot and (b) surface plot.

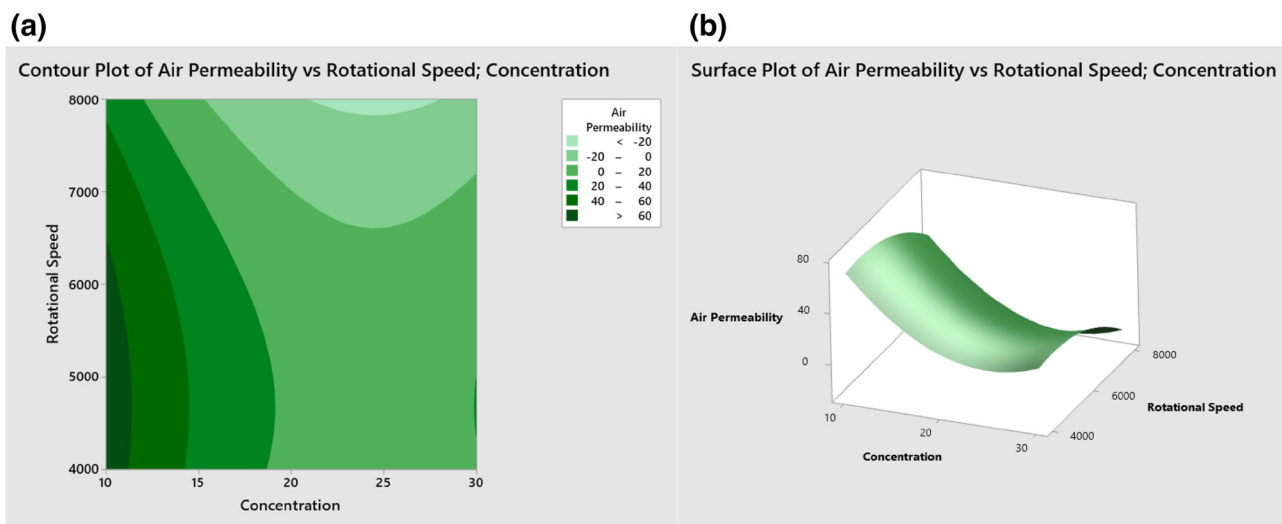


Figure 7. The effect of concentration and rotational speed on air permeability: (a) contour plot and (b) surface plot.

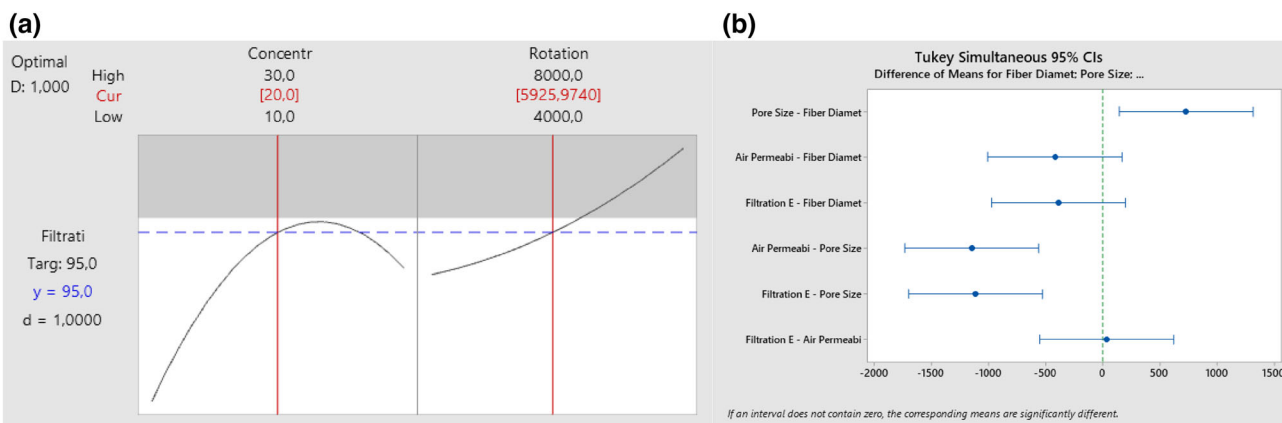


Figure 8. (a) Optimum process parameters, and (b) Tukey test result.

conditions to reach 95% filtration efficiency, coherent with the experimental results. Tukey test shows (figure 8b) that the difference between fiber diameter, pore size, air permeability and filtration efficiency is statistically significant and does not include zero.

#### 4. Conclusions

Gelatin nanofiber webs were successfully fabricated via centrifugal spinning technique with the changing diameter of 232 to 778 nm. When their air permeability and filtration efficiency were evaluated, it was seen that as filter media, gelatin nanofiber webs reached 95% filtration efficiency, which is the requirement of the N95 filter. From this standpoint, gelatin nanofiber can be used as N95 filtration media. Under the intense usage of facial and surgical masks, partially biomaterial containing mask material is an environmentally friendly option on the way of fully biodegradable mask fabrications. Further studies should aim to improve the strength of gelatin nanofibers to develop 100% degradable mask designs that can be used as a filtration material without the need for synthetic layers.

#### Acknowledgements

This research was funded by The Scientific and Technological Research Council of Turkey (TUBITAK) (TEY-DEB-1507), Project number 7200424. We would like to thank Halavet Gelatin, Turkey, for their gelatin supply.

#### References

- [1] Bałazy A, Toivola M, Adhikari A, Sivasubramani S K, Reponen T and Grinshpun S A 2006 *Am. J. Infect. Control* **34** 51
- [2] WHO Coronavirus (COVID-19) Dashboard. Available: <https://covid19.who.int/> (accessed on 07 July 2021)
- [3] Feng S, Shen C, Xia N, Song W, Fan M and Cowling B 2020 *J. Lancet Respir. Med.* **8** 434
- [4] Yim W, Cheng D, Patel S H, Kou R, Meng Y S and Jokerst J V 2020 *ACS Appl. Mater. Interfaces* **12** 54473
- [5] Shokraei S, Mirzaei E, Shokraei N, Derakhshan M A, Ghanbari H and Faridi M R 2021 *J. Appl. Polym. Sci.* **138** 50547
- [6] Ismar E and Sarac A S 2016 *Polym. Adv. Technol.* **27** 1383
- [7] Yang A, Cai L, Zhang R, Wang J, Hsu P C, Wang H *et al* 2017 *Nano Lett.* **17** 3506
- [8] Daniel N R 2021 *Int. J. Non-linear Mech.* **92** 1
- [9] Boran G and Regenstien J M 2009 *J. Food Sci.* **74** 432
- [10] Zhou P and Regenstien J M 2005 *J. Food Sci.* **70** c392
- [11] Gómez-Estaca J, Montero P, Fernández-Martín F and Gómez-Guillén M C 2009 *J. Food Eng.* **90** 480
- [12] Brinckmann J, Notbohm H and Müller P K 2005 *Collagen: primer in structure, processing and assembly* (Berlin Heidelberg: Springer-Verlag) pp 247–254
- [13] Echave M C, Burgo S L, Pedraz L J and Orive G 2017 *Curr. Pharm. Des.* **23** 3567
- [14] Huang T, Tu Z, Shangguan X, Sha X, Wang H, Zhang L *et al* 2019 *Trends Food Sci. Technol.* **86** 260
- [15] Nur Hanani Z A, Roos Y H and Kerry J P 2014 *Int. J. Biol. Macromol.* **71** 94
- [16] Zhang Y Z, Venugopal J, Huang Z M, Lim C T and Ramakrishna S 2006 *Polymer* **47** 2911
- [17] Huang Z M, Zhang Y Z, Ramakrishna S and Lim C T 2004 *Polymer* **45** 5361
- [18] Kadam V, Truong Y B, Schutz J, Kyratzis I L, Padhye R and Wang L J 2021 *Hazard. Mater.* **403** 123841
- [19] Souzandeh H, Wang Y and Zhong W H 2016 *RSC Adv.* **6** 105948
- [20] Fang Y, Dulaney A R, Gadley J, Maia J and Ellison C J 2016 *Polymer* **88** 102
- [21] Zhang Z M, Duan Y S, Xu Q and Zhang B 2019 *J. Eng. Fibers Fabr.* **14** 11
- [22] Gaitonde V N, Manjaiah M, Maradi S, Karnik S R, Petkar P M and Davim J P 2017 In *Computational methods and production engineering* (Elsevier Science: Woodhead Publishing) 1 244
- [23] Zhang X and Lu Y 2014 *Polym. Rev.* **54** 677
- [24] Li Z, Mei S, Dong Y, She F and Kong L 2019 *Polymers* **11** 1550
- [25] Aoki H, Miyoshi H and Yamagata Y 2015 *Polym. J.* **47** 267
- [26] Das M P, Suguna P R, Prasad K, Vijayalakshmi J V and Renuka M 2017 *Int. J. Pharm.* **9** 239
- [27] Kuppam P, Sethuraman S and Krishnan U M 2013 *J. Biomed. Nanotechnol.* **9** 1540
- [28] Sabantina L, Wehlage D, Klöcker M, Mamun A, Grothe T, García-Mateos F J *et al* 2018 *J. Nanomater.* **2018** 6131085
- [29] Kim S E, Heo D N, Lee J B, Kim J R, Park S H, Jeon S H *et al* 2009 *Biomed. Mater.* **4** 044106
- [30] Jakir Hossain M D, Gafur M A, Kadir M R and Karim M M 2014 *Int. J. Eng. Technol.* **14** 24
- [31] Azizi M, Azimzadeh M, Afzali M, Alafzadeh M and Mirhosseini S H 2018 *J. Adv. Mater. Process.* **6** 34
- [32] Chang D Q, Chen S C, Fox A R, Viner A S and Pui D Y H 2015 *Aerosol. Sci. Technol.* **49** 966
- [33] Lee S A, Hwang D C, Li H Y, Tsai C F, Chen C W and Chen J K 2016 *J. Healthc. Eng.* **2016** 12
- [34] Santra P K, Singh A K, Kulkarni G U, Kundu S, Rao T S and Ganesha M K 2021 *Energy Technol.* **2021** 2100614
- [35] Morrison S, Sosnoff J J, Heffernan K S, Jae S Y and Fernhall B 2013 *J. Neurol. Sci.* **326** 68
- [36] Al-Hassan A A and Norziah M H 2012 *Food Hydrocoll.* **26** 108
- [37] Sancakli A, Basaran B, Arican F and Polat O 2021 *SN Appl. Sci.* **3** 1